The porcine large intestine contains developmentally distinct submucosal lymphoid clusters and mucosal isolated lymphoid follicles

Jørgensen, Peter B.; Eriksen, Lise L.; Fenton, Thomas M.; Bailey, Michael; Agace, William W.; Mörbe, Urs M.

Published in:
Developmental and Comparative Immunology

Link to article, DOI:
10.1016/j.dci.2022.104375

Publication date:
2022

Document Version
Publisher's PDF, also known as Version of record

Developmental and Comparative Immunology 131 (2022) 104375

Contents lists available at ScienceDirect

Developmental and Comparative Immunology

journal homepage: www.elsevier.com/locate/devcompimm

The porcine large intestine contains developmentally distinct submucosal lymphoid clusters and mucosal isolated lymphoid follicles

Peter B. Jørgensen [a,1], Lise L. Eriksen [a,1], Thomas M. Fenton [a], Michael Bailey [b], William W. Agace [a,c], Urs M. Mörbe [a,*]

[a] Department of Health Technology, Technical University of Denmark, Kemitorvet, 2800 Kgs., Lyngby, Denmark
[b] Bristol Veterinary School, University of Bristol, Langford House, Langford, Bristol, BS40 5DU, UK
[c] Immunology Section, Lund University, BMC D14, Lund, Sweden

ARTICLE INFO

Keywords:
Gut-associated lymphoid tissue
Immune development
Pigs
Isolated lymphoid follicles

ABSTRACT

Gut-associated lymphoid tissues (GALT) serve as key priming sites for intestinal adaptive immune responses. Most of our understanding of GALT function and development arises from studies in mice. However, the diversity, structure and cellular composition of GALT differs markedly between mammalian species and the developmental window in which distinct GALT structures develop in large mammals remains poorly understood. Given the importance of pigs as models of human disease, as well as their role in livestock production, we adapted a recently developed protocol for the isolation of human GALT to assess the diversity, development and immune composition of large intestinal GALT in neonatal and adult pigs. We demonstrate that the large intestine of adult pigs contains two major GALT types; multifollicular submucosal GALT that we term submucosal lymphoid clusters (SLC) which develop prenatally, and as yet undescribed mucosal isolated lymphoid follicles (M-ILF), which arise after birth. Using confocal laser microscopy and flow cytometry, we additionally assess the microanatomy and lymphocyte composition of SLC and M-ILF, compare them to jejunal Peyer's patches (PP), and describe the maturation of these structures.

Collectively, our results provide a deeper understanding of the diversity and development of GALT within the porcine large intestine.

1. Introduction

Gut-associated lymphoid tissues (GALT) are organized secondary lymphoid tissues within the intestinal lining, which function as local immune-priming sites for the generation of intestinal effector lymphocytes, such as cytokine-producing T cells and IgA-secreting plasma cells (Fenton et al., 2020; Senda et al., 2019). The best-described GALT are the multifollicular Peyer's Patches (PP) of the small intestine, which in mice and humans develop before birth and accommodate large germinal centers, thereby contributing to intestinal IgA antibody responses (Fenton et al., 2020; Hashizume et al., 2008; Martinoli et al., 2007; Nagai et al., 2007). Additional isolated lymphoid follicles (ILF), each consisting of a single immune cell-rich follicle, can be found in the small and large intestines of mammals including humans (Fenton et al., 2020) and mice (Kanamori et al., 1996). The cellular composition and time frame of ILF development differs substantially between species (reviewed in (Mörbe et al., 2021)). For example, murine ILF are only present within the mucosa, develop around weaning (Kanamori et al., 1996; Hamada et al., 2002), consist of a central B cell cluster surrounded by a ring of group 3 innate lymphoid cells (ILC3), and mainly contribute to T cell-independent B cell responses (Tsuji et al., 2008; Pabst et al., 2006). In contrast, at least some human ILF develop before birth (Gustafson et al., 2014; Russell et al., 1990), they contain high numbers of T cells (Fenton et al., 2020; Senda et al., 2019), and can support germinal center reactions (Fenton et al., 2020; Magri et al., 2017). Furthermore, ILF in humans are located either within the mucosa (M-ILF) or penetrating the submucosa (SM-ILF). The numbers of these distinct structures also differ along the length of the intestine, with M-ILF dominating in the distal small intestine and SM-ILF dominating in the proximal colon (Fenton et al., 2020; Jørgensen et al., 2021; Moghaddami et al., 1998). However, whether M-ILF and SM-ILF arise within a similar or a distinct developmental time window remains unclear.

* Corresponding author.
E-mail address: mimurs@dtu.dk (U.M. Mörbe).
[1] These authors contributed equally.

https://doi.org/10.1016/j.dci.2022.104375
Received 11 October 2021; Received in revised form 13 February 2022; Accepted 13 February 2022
Available online 25 February 2022

In addition to mice, pigs have been used as large, long-lived and omnivorous mammalian models to study GALT (Pabst, 2020; Meurens et al., 2012). Porcine GALT include discrete jejunal PP with clear T cell zones and are thought to be a key contributor to T cell-dependent IgA responses in the intestine (Levast et al., 2010). Additionally, pigs possess a continuous ileal PP that might also serve as primary lymphoid organ (Andersen et al., 1999; Furukawa et al., 2020) and which has no direct counterpart in mice and humans, as well as "lymphoglandular complexes" (Morfitt and Pohlenz, 1989; Mansfield and Gauthier, 2004) in the large intestine, which are poorly studied lymphocyte-rich tissues along the porcine colon (Morfitt and Pohlenz, 1989; Mansfield and Gauthier, 2004). However, many questions around the exact anatomy, functions and development of these structures remain. Here we applied techniques that we recently developed to identify and study human GALT (Jørgensen et al., 2021), to assess GALT diversity, structure and composition within the porcine large intestine. Our results demonstrate that the porcine large intestine contains two major GALT structures; large multifollicular submucosal structures which we term multifollicular submucosal lymphoid clusters (SLC) and are anatomically similar to jejunal PP, and previously undescribed monofollicular structures reminiscent of human M-ILF. Interestingly, SLC were present in the large intestines of neonatal piglets, but M-ILF were absent, indicating that these distinct GALT have different developmental programs. Together, our results extend our understanding on the diversity, development and maturation of the porcine intestinal immune system and outlines similarities and differences to human GALT.

2. Materials and methods

2.1. Biological specimens

The pigs used in this study were derived from Danish breeding facilities following a specific pathogen free (SPF) sanitary strategy according to the guidelines of the Ministry of Environment and Food in Denmark. Intestinal tissues of adult Danish Landrace pigs (approximately 5-month-old) were obtained from a local abattoir after pigs were slaughtered for meat processing. Following slaughtering, full intestines and surrounding mesenterium were obtained from the slaughterhouse and processed within 2 h (h). Neonatal piglets (≤ 1 day after birth) were killed on the farm of origin by the breeder and full intestines with surrounding mesenterium were obtained. In this study, we focused on GALT in the distal porcine colon/rectum (25–50 cm distal from the rectal sphincter) and surrounding lamina propria (LP), since this area contains the highest GALT numbers in the large intestine (Morfitt and Pohlenz, 1989; Biswal et al., 1954). Parts of jejunum containing macroscopically visible discrete PP were taken from positions at least 100 cm away from the ileocaecocolic junction (to avoid the continuous ileal PP). Both male and female pigs were used for this study.

2.2. General tissue preparation

Intestinal lymphoid tissues were prepared using a modification of a protocol for the isolation of GALT from human intestinal tissues (Jørgensen et al., 2021) (Table S1). In short, approximately 20 cm^2 of small and large intestinal tissues were resected, the intestinal tube opened longitudinally, and gut content removed by washing tissues in cold R5 medium (Roswell Park Memorial Institute (RPMI) 1640 medium with 5% fetal calf serum (FBS), 100 units/mL penicillin and 100 μg/mL streptomycin (all from Thermo Fisher, Waltham, USA). Subsequently, the muscularis externa was removed using forceps and scissors, and the remaining tissue containing mucosa and submucosa (SM) washed twice in R5 buffer containing 4 mM Dithiothreitol (DTT; Thermo Fisher, Waltham, USA) for mucus removal. At this step, some tissue was taken for downstream histological processing and fixed for 6–12 h in phosphate-buffered saline (PBS; Thermo Fisher, USA) containing 4% paraformaldehyde (PFA; Sigma-Aldrich, St. Louis, USA) before transferring the fixed tissues into histology washing buffer (PBS with 5% FBS, 0.2% Triton-X100 (Sigma-Aldrich, St. Louis, USA), 0.01% thimerosal (Sigma-Aldrich, St. Louis, USA)) and stored until further use at 4 °C. Of the remaining tissue, the LP was carefully separated from the SM under a stereo microscope using two forceps. However, the colonic SM was peeled off in two steps due to its thickness; the outer fatty SM was first roughly peeled off, revealing underlying SLC, before the thin inner SM with the muscularis mucosa was separated from the LP. LP and SM layers were then screened for GALT as described previously (Jørgensen et al., 2021), and GALT counted and collected for enzymatic digestion. Meanwhile, isolated LP of adult pigs and neonate piglets was washed once in Hanks' Balanced Salt Solution (HBSS; Thermo Fisher, Waltham, USA) and 3–4 more times in HBSS containing 5 mM Ethylenediaminetetraacetic acid (EDTA; Thermo Fisher, Waltham, USA) for 10 min (min) at 37 °C and 370 rpm on an orbital shaker to remove the intestinal epithelial layer. To obtain single-cell suspensions for flow cytometry analysis, LP was cut into 2–3 mm^2 sections prior to digestion and tissues incubated in 5 mL digestion buffer (R5 with 40 μl/mL collagenase D (Sigma-Aldrich, St. Louis, USA) and 30 mg/mL DNase I (Roche, Basel, Switzerland)) for 45 min at 37 °C and 370 rpm on an orbital shaker. After enzymatic digestion, single-cell suspensions were washed once in R5 medium and frozen at −80 °C in freezing medium (50% FBS, 40% R5, 10% dimethyl sulfoxide (DMSO; MP Biomedicals, Santa Ana, USA) until further use.

2.3. Histological analysis

Fixed intestinal tissues were prepared for hematoxylin and eosin (H&E) staining and for confocal laser microscopy as described previously (Fenton et al., 2020; Jørgensen et al., 2021). In short, for H&E staining, tissues were embedded in paraffin, sectioned into 3 μm sections, stained on glass slides with H&E and analyzed using a microscope/camera system (DMLS/DFC290; Leica, Wetzlar, Germany). For confocal laser microscopy analysis, fixed tissues were either directly stained and cleared or embedded in 4% low melting agarose and sectioned into 50–80 μm sections with a swinging blade microtome (VT1200S; Leica, Wetzlar, Germany). For the former, tissues were incubated with fluorescently-labelled antibodies indicated in Table S2 for >24 h in histology washing buffer. Cell nuclei were stained for 10 min with 4′,6-diamidino-2-phenylindole (DAPI; Thermo Fisher, Waltham, USA) in histology washing buffer. Stained tissues were cleared by immersion in iohexol (Omnipaque ™, GE Healthcare, Chicago, USA) for 24 h, mounted on a glass slide in iohexol and imaged within 24 h. To image sectioned tissues, sections were stained with the unconjugated or fluorescently-labelled antibodies indicated in Table S2. Unconjugated antibodies were detected with fluorescently labelled secondary antibodies shown in Table S2 during a >2 h additional incubation in histology washing buffer, cell nuclei were stained using DAPI. Stained tissue sections were washed in histology washing buffer and mounted on glass slides using ProLong Gold (Thermo Fisher, Waltham, USA) mounting medium. Mounted samples were imaged using an LSM710 confocal laser microscope (Carl Zeiss, Jena, Germany) and acquired images analyzed using the Zeiss Zen software v2.3 (Carl Zeiss, Jena, Germany) and Imaris v8 (Oxford Instruments, Abingdon, UK) (Table S3).

2.4. Flow cytometry analysis

For flow cytometry analysis, frozen cells were thawed, washed once in R5 and blocked with PBS containing 2% FBS and 3% mouse serum for 10 min at 4 °C to prevent unspecific antibody binding. Cells were subsequently stained in PBS with 2% FBS containing the indicated antibodies in Table S2 for 30 min at 4 °C. 7-Amino-Actinomycin D (7-AAD; Biolegend, San Diego, USA) was added at least 5 min before flow cytometry analysis to detect dead cells. Cells were analyzed using an LSRFortessa (BD Biosciences, Franklin Lakes, USA), and generated data

analyzed using FlowJo software v10.7.1 (BD Biosciences, Franklin Lakes, USA; Table S3).

2.5. Statistical analysis

All statistical analyses were performed using R version 3.5.1 (R Studio, Boston, Massachusetts) or GraphPad Prism version 9.0.2 (GraphPad, San Diego, USA; Table S3). For Fig. 3D and E, a Mann-Whitney test was used. For Fig. 4C, a 2-way ANOVA with Sidak's multiple comparisons test was performed. Results with a p-value <0.05 were considered statistically significant, asterisks indicate statistical significance as following: *p $\leq$ 0.05, **p $\leq$ 0.01, ***p $\leq$ 0.001, ****p $\leq$ 0.0001.

3. Results

3.1. The large intestine of adult pigs contains multifollicular submucosal lymphoid clusters and mucosal isolated lymphoid follicles

To assess the structure, organization and cellular composition of porcine GALT, we adapted our recently published protocols for the isolation of human GALT (Jørgensen et al., 2021) to pig intestines. This isolation technique allowed us to identify and isolate distinct porcine GALT structures within the pig large and small intestinal LP as well as in the SM. Histological analysis of the porcine distal large intestine revealed the presence of multifollicular lymphoid structures (Fig. 1A), which likely represent the poorly described "lymphoglandular complexes", which were described several decades ago in the porcine colon (Morfitt and Pohlenz, 1989; Mansfield and Gauthier, 2004; Biswal et al., 1954). Given their anatomy, localization within the intestinal wall, and the observation that these structures are densely packed with lymphocytes but seem to lack *bona fide* glandular tissue (Morfitt and Pohlenz, 1989; Mansfield and Gauthier, 2004), we considered them GALT and

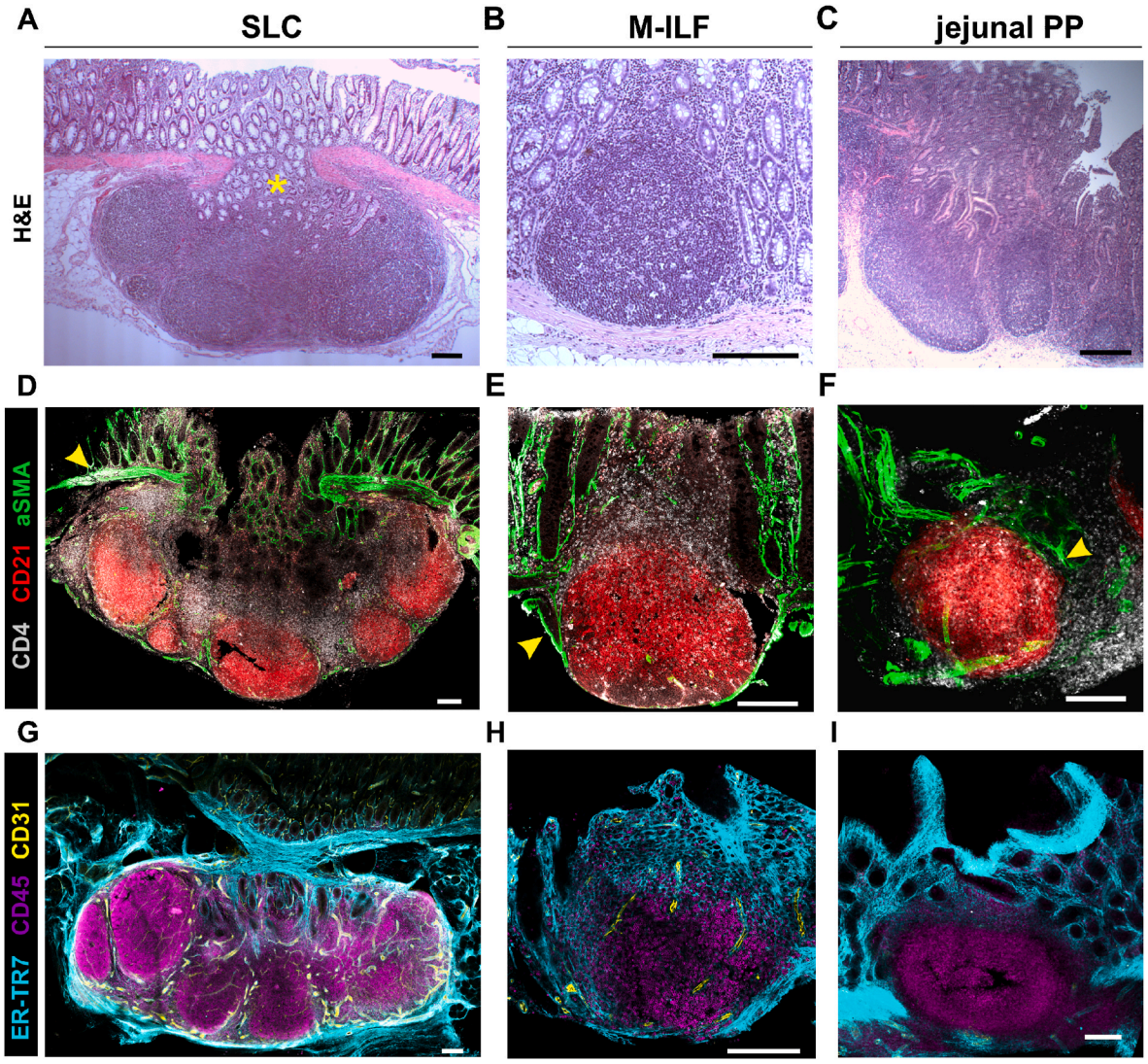

Fig. 1. Histological characterization of adult porcine GALT. (A–C) Images of H&E staining of a colonic SLC (A), a colonic M-ILF (B), and a jejunal PP (C) derived from an adult pig. (D–F) Confocal laser microscopy images showing the organization of GALT including a colonic SLC (D), a colonic M-ILF (E), and a jejunal PP (F) of an adult pig. $CD21^+$ B cells shown in red, $CD4^+$ T cells shown in white. Their position within the gut wall is shown in relation to the alpha smooth muscle actin $(\alpha SMA)^+$ (green) muscularis mucosa (yellow arrows). (G–I) Confocal laser microscopy images of colonic GALT showing $CD45^+$ lymphocyte-rich follicles (magenta), the presence of $CD31^+$ vessels (yellow) and ER-$TR7^+$ fibroblastic reticular cells (turquoise). Panels show SLC (G), M-ILF (H), and jejunal PP (I). (A–I) One representative image shown from $\geq$ three individual replicates of individual pigs. Scale bars represent 200 μm.

subsequently termed them submucosal lymphoid clusters (SLC). While the present study and previous studies (Morfitt and Pohlenz, 1989; Mansfield and Gauthier, 2004) indicate that SLC are located primarily within the SM, our imaging showed that these structures possess a centrally-located "funnel-like" protrusion into the intestinal LP, providing a direct interface between the lymphoid tissue and the intestinal LP. These funnels penetrated the muscularis mucosa and coincided with the presence of intestinal crypts within the lymphoid organ (Fig. 1A). While we detected no other multifollicular GALT in the mucosa of the porcine distal colon, we also identified substantially smaller isolated lymphoid follicles within the LP which did not penetrate the muscularis mucosa (Fig. 1B, S1A-B). Since the location of these structures was similar to the M-ILF we recently described in the human intestine, we termed them porcine M-ILF. For comparison, we also analyzed isolated PP from the porcine jejunum (Fig. 1C) and confirmed anatomical similarities to the SLC in regard to their location within the gut wall and their multifollicular organization.

3.2. SLC and M-ILF in adult pigs are highly organized lymphocyte reservoirs

To assess the organization of porcine large intestinal GALT in further detail, tissue sections of SLC and M-ILF were stained for the presence of $CD45^+$ lymphocytes, $CD4^+$ T cells, $CD21^+$ B cells, αSMA^+ smooth muscle cells, $CD31^+$ endothelial cells and $ER\text{-}TR7^+$ mesenchymal stromal cells (Van Vliet et al., 1986) and analyzed by confocal laser microscopy (Fig. 1D–I). Consistent with our H&E staining (Fig. 1A), SLC penetrated the αSMA^+ muscularis mucosa, bringing them in direct proximity to the gut lumen, while colonic M-ILF did not breach the muscularis mucosa layer (Fig. 1D–F). Similar to porcine isolated jejunal PP, SLC of adult pigs contained multiple marginal B cell follicles as well as large perifollicular and central T cell areas (Fig. 1D and F). In contrast, M-ILF contained a single isolated central B cell follicle (Figs. 1E and S1B) with a peripheral T cell zone (Fig. 1E). The organ parenchyma and margins of GALT structures additionally contained $CD31^+$ vessels present primarily at perifollicular locations and a fibroblast network marked by the monoclonal ER-TR7 antibody (Van Vliet et al., 1986; Katakai et al., 2004), highlighting fibroblast-derived reticular fibers consisting of collagen IV (Schiavinato et al., 2021) (Fig. 1G–I). Together these findings demonstrate that porcine GALT are composed of the same basic building blocks observed in human multi-follicular GALT and M-ILF (Fenton et al., 2020; Mörbe et al., 2021; Junt et al., 2008).

Finally, we also observed low numbers of isolated follicles in the colonic SM and muscularis mucosa (Fig. S1D). These structures were approximately the same size range as porcine M-ILF (Fig. S1E) and of human submucosal ILF (SM-ILF) (Fenton et al., 2020): however, at this point it remains unclear whether these structures truly represent SM-ILF or, rather, M-ILF that were separated with the muscularis mucosa during the separation of the LP from the SM.

3.3. Flow cytometry reveals the lymphocyte composition of porcine GALT

To obtain insights into the lymphocyte composition of porcine GALT, single-cell suspensions of GALT and surrounding LP were prepared and analyzed by flow cytometry (Fig. S2A). Almost all live cells obtained from GALT were $CD45^+$ (Fig. S2B) and thus hematopoietic in origin. GALT-derived $CD45^+$ cells consisted primarily of $CD21^+$ B cells and $CD3^+$ T cells. $CD21^{hi}$ cells were enriched in GALT compared to the surrounding colonic LP (Fig. 2A–B), in line with findings that CD21 expression is high on naïve and primed B cells, but lower on LP plasma cells (Sinkora et al., 2013, 2014). Most $CD3^+$ T cells in porcine GALT expressed CD4 and low levels of CD8 (Fig. 2B), suggesting that these cells represent functionally mature T helper cells (Gerner et al., 2009; Pescovitz et al., 1994; Zuckermann and Gaskins, 1996). Conversely, LP $CD3^+$ T cells were enriched for $CD4^-CD8^+$ T cells and $CD4^-CD8^-$ double negative cells (Fig. 2B), which have been suggested to represent

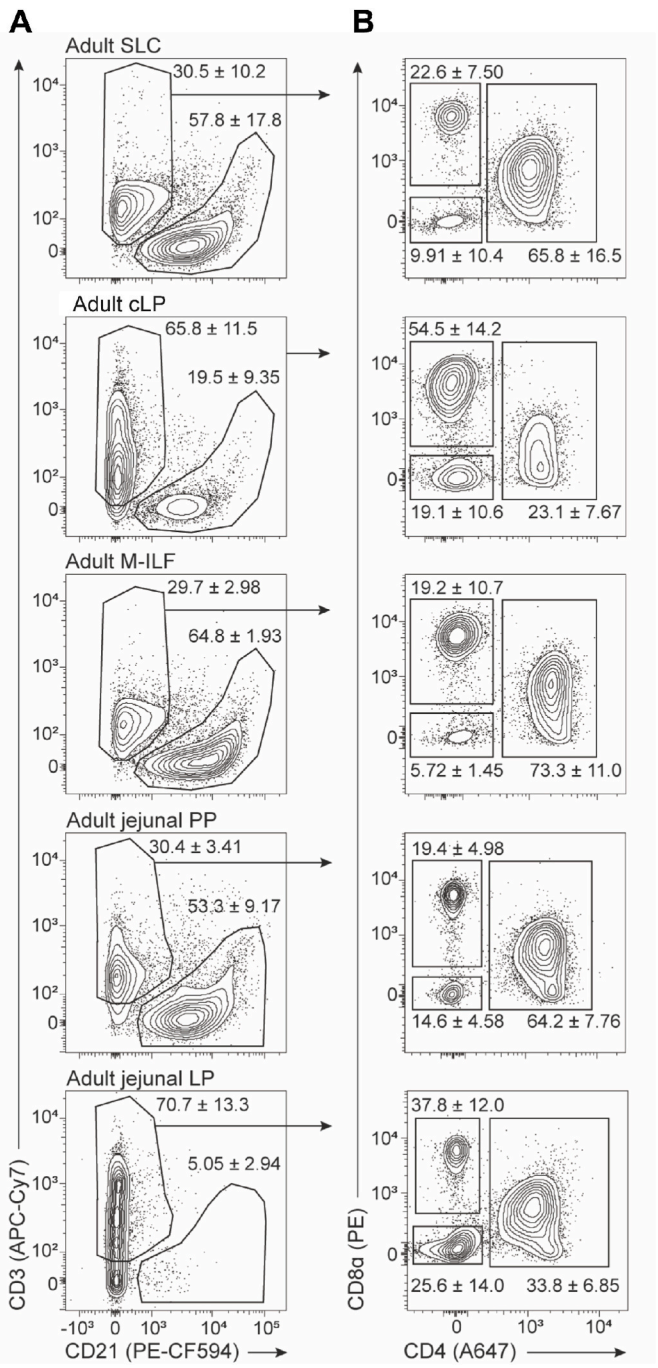

Fig. 2. Flow cytometry analysis of intestinal lymphocytes of adult pigs. (A) $CD45^+$ cells and (B) $CD3^+$ T cells isolated from the indicated intestinal locations of adult pigs. Numbers indicate means ± 1 SD from 3 to 8 individual pigs and 3 individual experiments.

porcine effector cytotoxic T lymphocytes (Gerner et al., 2009; Zuckermann and Gaskins, 1996) and γδ T cells (Boeker et al., 1999; Yang and Parkhouse, 1996), respectively.

Together, our data demonstrate that porcine large intestinal GALT constitute dedicated lymphocyte reservoirs with a similar organization as porcine small intestinal PP, and a lymphocyte composition distinct to that of the surrounding LP.

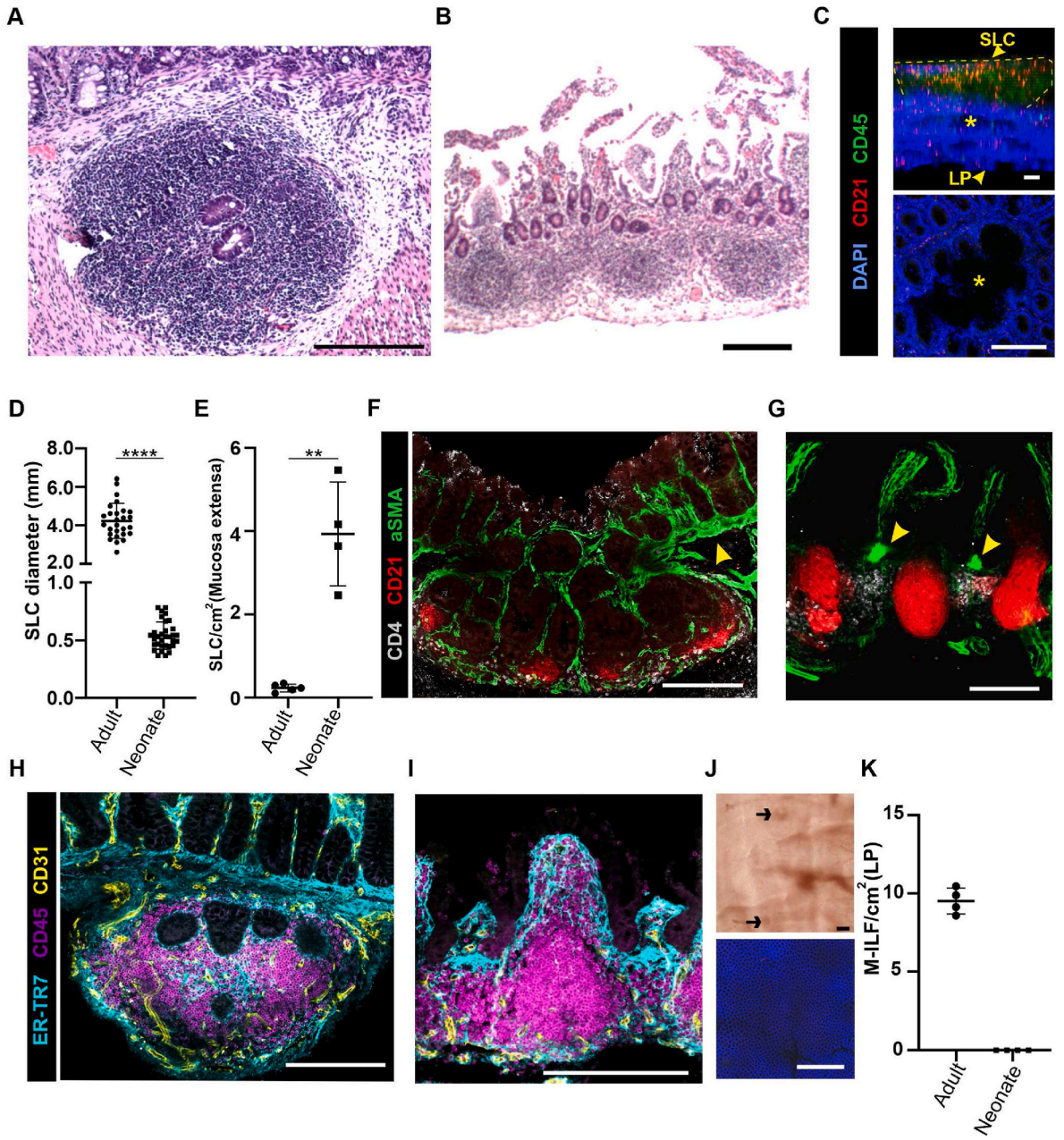

Fig. 3. The GALT compartment of neonate piglets. (A–B) H&E staining of a colonic SLC (A) and a discrete jejunal PP (B) derived from a neonate piglet. (C) Confocal laser microscopy images of a cleared, neonate piglet-derived SLC. Images show the CD45$^+$ lymphocyte cluster (green) including CD21$^+$ B cells (red) located in the submucosa (SM, left panel), as well as the underlying LP highlighted by a DAPI$^+$ cell layer low in CD45$^+$/CD21$^+$ lymphocytes, but with a funnel-like interface between SLC and gut lumen (asterisk). Dotted yellow line marks the SLC margins within the intestinal submucosa. Representative image out of 20 SLC derived from 4 individual neonate piglets. (D–E) Measurement of follicle size in the adult and neonate porcine colonic SM. Each dot represents an SLC derived from 5 (adult) or 4 (neonate) individual pigs. (E) Quantification of follicles in the adult (5 animals) and neonate (4 animals) porcine colonic SM. (F–G) Confocal laser microscopy image showing the organization of SLC (F) and jejunal PP (G) in neonate piglets containing CD21$^+$ B cells (red) and CD4$^+$ T cells (white) as well as their position in the gut wall in relation to the αSMA$^+$ (green) muscularis mucosa (yellow arrows). (H–I) Confocal laser microscopy image of colonic SLC (H) and jejunal PP (I) showing CD45$^+$ lymphocyte-rich follicles (magenta), the presence of CD31$^+$ vessels (yellow) and fibroblasts highlighted by the ER-TR7 antibody (turquoise). (J) Analysis of neonate piglet LP showing the absence of M-ILF. Upper panel shows bright field image of LP from a neonate piglet, arrows mark LP invaginations of underlying SLC. Scale bars = 2 mm. Lower panel shows cleared confocal laser microscopy image of intestinal LP of a neonate pig. Scale bar = 1 mm. (K) Enumeration of M-ILF in the LP of adult and neonate pig large intestines. (A-C, F–I) Scale bars in (A-C, F–I) represent 200 μm. Images shown in (A-B, F-J) are representative images out of ≥3 replicates from individual neonate piglets.

3.4. The intestine of neonate piglets contains multifollicular SLC, but no M-ILF

Since PP and ILF in mice have been shown to arise during different developmental time windows (Hamada et al., 2002; Baptista et al., 2013; Veiga-Fernandes et al., 2007), we next assessed whether porcine GALT are present in neonatal piglets. Similar to adult pigs (Fig. 1), we detected large GALT including SLC in the large intestinal submucosa, with crypt-like structures in the parenchyma (Fig. 3A) and discrete jejunal PP (Fig. 3B). In these neonatal piglets, SLC already possessed "funnel-like" protrusions into the LP (Fig. 3C). Neonatal SLC were substantially smaller than their counterparts in adult pigs (Fig. 3D), but

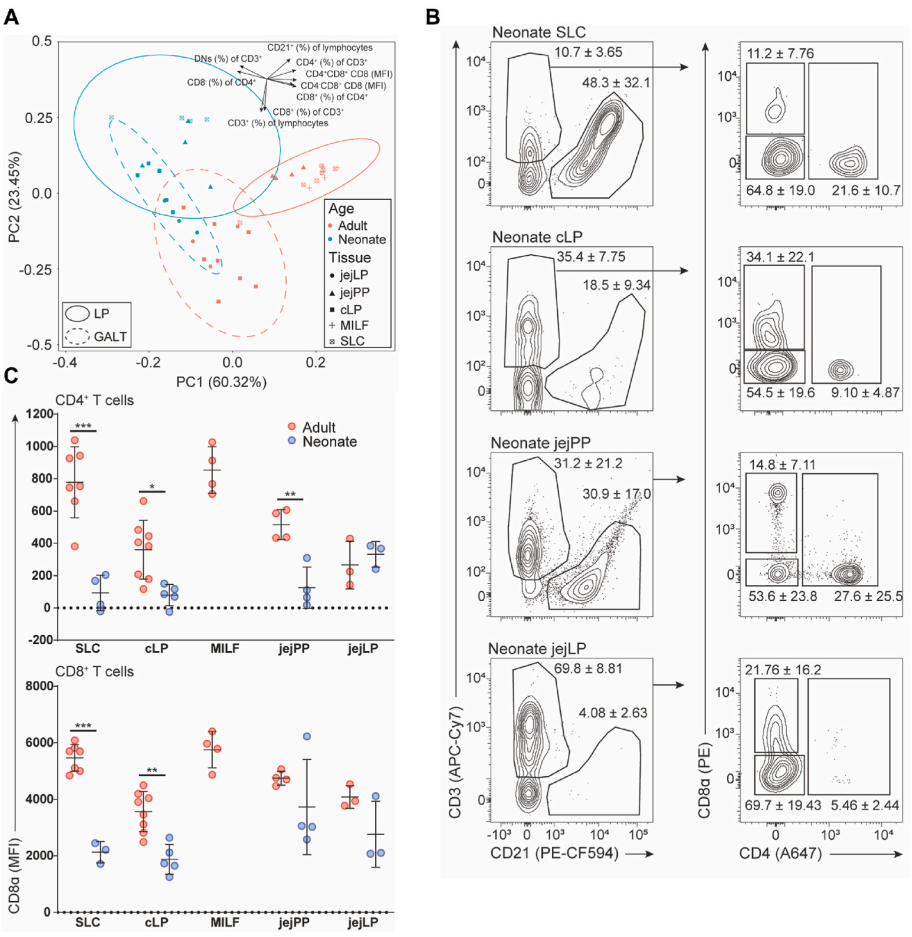

Fig. 4. Flow cytometry assessment of neonatal porcine GALT and LP. (A) Principal component analysis of all recorded flow cytometry parameters including all analyzed samples, each dot represents one individual sample. Considered flow cytometry parameters include expression of CD21, CD3, CD4 and CD8, as well as mean fluorescence intensities of the analyzed factors. Lines and dotted lines indicate statistical ellipses' at 95% confidence intervals of GALT (jejPP, SLC and/or MILF) and LP (cLP and jejLP), respectively. Arrows indicate flow cytometry parameters driving principal component 1 and 2; see also Fig. S2A for parameters. cLP = colonic LP; jejLP = jejunum lamina propria; jejPP = jejunum Peyer's patch; MILF = mucosal isolated lymphoid follicle; SLC = submucosal lymphoid cluster. (B) Flow cytometry analysis of CD45$^+$ cells isolated from the indicated intestinal locations of neonate piglets. Left panels show the total CD45$^+$ gate, right panels show the CD3$^+$ T cell compartment. Numbers indicate means ± 1 SD from 3 to 5 individual pigs and 3 individual experiments. (C) Levels of CD8α expression by CD3$^+$CD4$^+$ T helper cells with (upper panel) and CD3$^+$CD4$^-$CD8$^+$ T lymphocytes (lower panel), with each individual dot representing an individual pig and with the mean and ±1 SD given.

were present in significantly higher densities (Fig. 3E), confirming that immature SLC form before birth (McCance, 1974; Skrzypek et al., 2018) and in line with the notion that the intestine grows extensively after birth (Skrzypek et al., 2018; Xu et al., 1992). Neonatal SLC, similar to neonatal PP (Furukawa et al., 2020; Barman et al., 1997; Makala et al., 2000), already contained multiple discrete CD21$^+$ B cell follicles but few CD4$^+$ T cells (Fig. 3F and G), indicating that the accumulation of these cells occurs after birth. CD31$^+$ endothelial cells and ER-TR7$^+$ mesenchymal stromal cells were also detectable in neonatal SLC (Fig. 3H) and jejunal PP (Fig. 3I), corroborating that the anlagen, i.e. the earliest developmental structure, of porcine multifollicular GALT develops before birth. In marked contrast to SLC, M-ILF were not observed in the neonatal porcine large intestine (Fig. 3J–K). To exclude the possibility that M-ILF anlagen within the LP of neonatal piglets were too small to be seen by conventional bright field microscopy, we additionally analyzed cleared whole-mount LP and confirmed the absence of these structures using confocal laser microscopy staining for accumulations of CD45$^+$ lymphocytes and CD21$^+$ B cells (Fig. 3J). Thus, SLC develop during embryogenesis, while M-ILF develop after birth.

3.5. The lymphocyte compartment within porcine GALT undergoes postnatal maturation

To compare the immune composition of GALT between neonatal and adult pigs, flow cytometry analysis was performed on neonatal and adult SLC, jejunal PP and surrounding LP, as well as on M-ILF of adult pigs. Principal component analysis (PCA) of CD21, CD3, CD4 and CD8 expression demonstrated that SLC, PP and M-ILF samples clustered together rather than with the surrounding LP in adult pigs (Fig. 4A), highlighting their distinct immune composition. In addition, neonatal and adult GALT clustered separately from each other, supporting the notion that porcine GALT undergoes substantial maturation after birth (Stokes, 2017; Bailey and Haverson, 2006; Bailey et al., 2005). Specifically, the flow cytometry analysis confirmed the histological findings that neonatal SLC and PP mainly contain CD21$^+$ B cells and few T cells (Fig. 4B). Expression of CD8 by CD3$^+$CD4$^+$ T helper and CD4$^-$ CD8$^+$ cytotoxic T cell subsets was also lower in neonates compared to adult GALT (Fig. 4C). Since CD8 is upregulated by antigen-experienced memory/effector T cells in pigs (Zuckermann and Gaskins, 1996; Zuckermann and Husmann, 1996; Dillender and Lunney, 1993), these results suggest that T cells in neonatal GALT are immature.

4. Discussion

Pigs offer a series of advantages as animal model over rodents regarding lymphoid tissue physiology and the generation of mucosal immune responses, including the presence of tonsils (Liebler-Tenorio and Pabst, 2006), similar pre- and postnatal immune compartment development and maturation (Bailey et al., 2005; Rothkötter et al., 2002), and the feasibility to follow immune responses over long periods of time (Meurens et al., 2012; Gerdts et al., 2015). However, the cellular composition, anatomy and development of large intestinal GALT in pigs remained poorly understood. In this study, we adapted our previously published protocols to isolate GALT from the human intestine to assess these structures in neonatal and adult pigs. Within the porcine distal colon, we found multifollicular SLC within the SM in accordance with previous findings (Morfitt and Pohlenz, 1989; Mansfield and Gauthier, 2004; Biswal et al., 1954), described their anatomy in detail, and showed that these structures are already present around birth. In addition, we identified as yet undescribed ILF within the large intestinal

mucosa of adult pigs, which each consisted of a single B cell follicle, and which developed after birth. In summary, our data highlight that both porcine SLC and M-ILF represent local intestinal leukocyte hubs with high densities of memory and effector-type lymphocytes; but with different developmental timelines.

As such, we believe that our work lays important groundwork for future studies using pigs as animal models to study GALT. We speculate that pigs could provide a useful model for GALT development as it remains difficult to study human GALT during early life, and there are major differences between murine and human ILF in regard to their cellular composition and development (reviewed in (Mörbe et al., 2021)). Using human intestinal resection material, we previously found that the distal large intestine of humans harbors a high density of mucosal and submucosal ILF with a size and immune cell compartment reminiscent of porcine M-ILF (Fenton et al., 2020; Mörbe et al., 2021). In contrast, mice only harbor small mucosal ILF mainly consisting of a central B cell follicle with a surrounding ring of group 3 innate lymphoid cells and only few T cells (Hamada et al., 2002; Tsuji et al., 2008; Kiss et al., 2011). Our analyses also showed that SLC were already present around birth, indicating that these organs develop in the sterile environment of the placenta during embryogenesis. Analogously, this was reported previously for at least some human ILF (Gustafson et al., 2014; Spencer et al., 2012) and we speculate that SLC could represent the porcine counterparts of such ILF, even though *bona fide* multifollicular GALT in the human colon are rare (Fenton et al., 2020). Unlike SLC, porcine M-ILF developed after birth in the early life of pigs. This characteristic is shared with murine ILF, which develop around weaning age (Kanamori et al., 1996) and mature in response to the intestinal microbiota (Bouskra et al., 2008). While the exact time point and drivers of M-ILF development in humans and pigs remain unknown, there is evidence that the numbers of total ILF in humans increase during the first months of life (Dukes and Bussey, 1926; Hellmann, 1921), compatible with our findings in pigs that M-ILF develop after birth.

Additionally, pigs could be useful to decipher the contributions of GALT to intestinal immune responses during infections (Meurens et al., 2012) or vaccinations (Meurens et al., 2012; Gerdts et al., 2015). Using human intestinal resection material, we previously showed that human GALT contribute to regionalized immune responses as there was a high overlap in the IgA^+ B cell repertoire between ileal PP and ileal LP, as well as between colonic SM-ILF and surrounding colonic LP, but to a substantially lesser extent between PP or SM-ILF and the respectively more distant LP site (Fenton et al., 2020). While this data is in agreement with findings that human PP and ILF harbor immune cell types associated with the presence of germinal centers, such as follicular dendritic cells (Fenton et al., 2020), T follicular helper cells (Fenton et al., 2020) and germinal center B cells (Fenton et al., 2020; Zhao et al., 2018), it is extremely difficult to study immune cell priming within human GALT in detail, as local immune responses can hardly be followed over time using human intestinal resection material or biopsies. We and others (Pabst, 2020; Meurens et al., 2012; Gerdts et al., 2015) therefore propose that pigs could provide an attractive model to overcome this hurdle. It has, for example, been shown previously that porcine SLC accommodate germinal centers contributing to local IgA responses during intestinal *Campylobacter jejuni* and *Trichuris suis* infection (Mansfield and Gauthier, 2004). Additionally, local delivery of fimbriae derived from enterotoxigenic *Escherichia coli* (*E. coli*) into the jejunal PP of pigs resulted in a local induction of antigen-specific IgA and IgM (Snoeck et al., 2006), together demonstrating the feasibility to delineate GALT contributions to intestinal immunity during immune challenges in pigs.

Finally, we speculate that a better understanding of GALT development in pigs could have implications for future livestock farming. For example, enterotoxigenic infection of young piglets by pathogenic *E. coli* strains (Fairbrother et al., 2005) or *Clostridium* spp. (Yaeger et al., 2002) are an important problem in the pork production industry causing extensive diarrhea in piglets, death of animals, and large economic losses (Fairbrother et al., 2005; Luppi, 2017; Rhouma et al., 2017). On the other hand, adult pigs are less susceptible to infection with pathogenic *E. coli* and *Clostridium* spp. (Yaeger et al., 2002; Dean-Nystrom and Samuel, 1994; Dean, 1990), a finding that could be explained by the extensive maturation process the porcine intestinal immune system undergoes after birth (own findings and (Furukawa et al., 2020; Bailey et al., 2005; Pabst et al., 1988)).

In conclusion, the present study provides novel data regarding the structure and development of the porcine intestinal immune system. Nevertheless, many open questions remain surrounding the function, development and diversity of porcine GALT. Importantly, the precise functions of GALT during immune challenges over time, and the functional differences between the GALT sites, both remain poorly understood. Regarding the latter, it should be noted that the intestinal tract of adult pigs spans approximately 23 m (Kararli, 1995), making it possible that other intestinal areas accommodate additional GALT. At this point it also remains unclear whether the small, rare, follicular structures that we found in the large intestinal SM represent putative porcine SM-ILF or simply parts of M-ILF stuck to the SM/muscularis mucosa layer during the process of physical separation of LP and SM. Lastly, the abundance of immune cells other than T and B cells in porcine GALT should be investigated further, for example in respect to professional antigen-presenting cells important to T cell priming (Johansson-Lindbom et al., 2003) and in regard to ILC3, which are crucially involved in the GALT development (reviewed in (Mörbe et al., 2021)). While future studies will have to clarify these questions in detail, we show that pigs provide a useful model to study large intestinal GALT, and we propose that these structures should be considered in future infection and vaccination approaches.

Author contributions

PBJ, LLE and UMM performed experiments and analyzed data. PBJ, WWA and UMM wrote the manuscript. UMM, PBJ, TMF and WWA conceived the study and discussed data, UMM coordinated experiments. MB discussed data, gave input on the manuscript and provided crucial reagents. All authors reviewed and approved the manuscript.

Declaration of competing interest

The authors declare no conflict of interest.

Acknowledgements

We thank Hans Hansen and Henrik Mortensen with the help to acquire intestinal samples from pigs. We also want to thank Rachel Burt (University of Bristol), who provided explanations and the MIL17 clone against porcine CD4. We thank Susanne Primdahl (DTU) for her help with H&E sectioning. We thank Peter Heegaard (DTU), Gitte Erbs, Jeanne Toft Jakobsen and Gregers Jungersen (all three at Statens Serum Institut) for valuable feedback during preparation of this manuscript. We thank Anders Reenberg Andersen (DTU) for help with the statistical analyses. This work was supported by a grant of the Lundbeck Foundation (R155-2014-4184) to William Agace.

Appendix A. Supplementary data

Supplementary data to this article can be found online at https://doi.org/10.1016/j.dci.2022.104375.

References

Andersen, J.K., Takamatsu, H., Oura, C.A., Brookes, S.M., Pullen, L., Parkhouse, R.E., 1999 Dec. Systematic characterization of porcine ileal Peyer's patch, I. apoptosis-sensitive immature B cells are the predominant cell type. Immunology 98 (4), 612–621.

Bailey, M., Haverson, K., 2006 May-Jun. The postnatal development of the mucosal immune system and mucosal tolerance in domestic animals. Vet. Res. 37 (3), 443–453.
Bailey, M., Haverson, K., Inman, C., Harris, C., Jones, P., Corfield, G., Miller, B., Stokes, C., 2005 Oct 18. The influence of environment on development of the mucosal immune system. Vet. Immunol. Immunopathol. 108 (1–2), 189–198.
Baptista, A.P., Olivier, B.J., Goverse, G., Greuter, M., Knippenberg, M., Kusser, K., Domingues, R.G., Veiga-Fernandes, H., Luster, A.D., Lugering, A., Randall, T.D., Cupedo, T., Mebius, R.E., 2013 May. Colonic patch and colonic SILT development are independent and differentially regulated events. Mucosal Immunol. 6 (3), 511–521.
Barman, N.N., Bianchi, A.T., Zwart, R.J., Pabst, R., Rothkötter, H.J., 1997 Jan. Jejunal and ileal Peyer's patches in pigs differ in their postnatal development. Anat. Embryol. 195 (1), 41–50.
Biswal, G., Morrill, C.C., Dorstewitz, E.L., 1954 Jan. Glands in the submucosa of the porcine colon. Cornell Vet. 44 (1), 93–102.
Boeker, M., Pabst, R., Rothkötter, H.J., 1999 Sep. Quantification of B, T and null lymphocyte subpopulations in the blood and lymphoid organs of the pig. Immunobiology 201 (1), 74–87.
Bouskra, D., Brézillon, C., Bérard, M., Werts, C., Varona, R., Boneca, I.G., Eberl, G., 2008 Nov 27. Lymphoid tissue genesis induced by commensals through NOD1 regulates intestinal homeostasis. Nature 456 (7221), 507–510.
Dean, E.A., 1990 Dec. Comparison of receptors for 987P pili of enterotoxigenic Escherichia coli in the small intestines of neonatal and older pig. Infect. Immun. 58 (12), 4030–4035.
Dean-Nystrom, E.A., Samuel, J.E., 1994 Nov. Age-related resistance to 987P fimbria-mediated colonization correlates with specific glycolipid receptors in intestinal mucus in swine. Infect. Immun. 62 (11), 4789–4794.
Dillender, M.J., Lunney, J.K., 1993 Jan. Characteristics of T lymphocyte cell lines established from NIH minipigs challenge inoculated with Trichinella spiralis. Vet. Immunol. Immunopathol. 35 (3–4), 301–319.
Dukes, C., Bussey, H.J.R., 1926. The number of lymphoid follicles of the human large intestine. J. Pathol. Bacteriol. 29, 111–116.
Fairbrother, J.M., Nadeau, E., Gyles, C.L., 2005 Jun. Escherichia coli in postweaning diarrhea in pigs: an update on bacterial types, pathogenesis, and prevention strategies. Anim. Health Res. Rev. 6 (1), 17–39.
Fenton, T.M., Jørgensen, P.B., Niss, K., Rubin, S.J.S., Mörbe, U.M., Riis, L.B., Da Silva, C., Plumb, A., Vandamme, J., Jakobsen, H.L., Brunak, S., Habtezion, A., Nielsen, O.H., Johansson-Lindbom, B., Agace, W.W., 2020 Mar 17. Immune profiling of human gut-associated lymphoid tissue identifies a role for isolated lymphoid follicles in priming of region-specific immunity. Immunity 52 (3), 557–570. *e6*.
Furukawa, M., Ito, S., Suzuki, S., Fuchimoto, D., Onishi, A., Niimi, K., Usami, K., Wu, G., Bazer, F.W., Ogasawara, K., Watanabe, K., Aso, H., Nochi, T., 2020 Dec 4. Organogenesis of ileal peyer's patches is initiated prenatally and accelerated postnatally with comprehensive proliferation of B cells in pigs. Front. Immunol. 11, 604674.
Gerdts, V., Wilson, H.L., Meurens, F., van Drunen Littel-van den Hurk, S., Wilson, D., Walker, S., Wheler, C., Townsend, H., Potter, A.A., 2015. Large animal models for vaccine development and testing. ILAR J. 56 (1), 53–62.
Gerner, W., Käser, T., Saalmüller, A., 2009 Mar. Porcine T lymphocytes and NK cells - an update. Dev. Comp. Immunol. 33 (3), 310–320.
Gustafson, C.E., Higbee, D., Yeckes, A.R., Wilson, C.C., De Zoeten, E.F., Jedlicka, P., Janoff, E.N., 2014 May. Limited expression of APRIL and its receptors prior to intestinal IgA plasma cell development during human infancy. Mucosal Immunol. 7 (3), 467–477.
Hamada, H., Hiroi, T., Nishiyama, Y., Takahashi, H., Masunaga, Y., Hachimura, S., Kaminogawa, S., Takahashi-Iwanaga, H., Iwanaga, T., Kiyono, H., Yamamoto, H., Ishikawa, H., 2002 Jan 1. Identification of multiple isolated lymphoid follicles on the antimesenteric wall of the mouse small intestine. J. Immunol. 168 (1), 57–64, 2002.
Hashizume, T., Togawa, A., Nochi, T., Igarashi, O., Kweon, M.N., Kiyono, H., Yamamoto, M., 2008 Mar. Peyer's patches are required for intestinal immunoglobulin A responses to Salmonella spp. Infect. Immun. 76 (3), 927–934.
Hellmann, T., 1921. Studien über das lymphoide Gewebe. IV. Zur Frage des Status lymphaticus. Untersuchungen über die Menge des lymphoiden Gewebes, besonders des Darmes beim Mensehen mittels einer quantitativen Bestimmungsmethode. Zeitschr. f. d. ges. Anat., II. kbt.: Zeitschr. f. Konstitutionsl. Bd. 8, 191–219. H. 3, S.
Johansson-Lindbom, B., Svensson, M., Wurbel, M.A., Malissen, B., Márquez, G., Agace, W., 2003 Sep 15. Selective generation of gut tropic T cells in gut-associated lymphoid tissue (GALT): requirement for GALT dendritic cells and adjuvant. J. Exp. Med. 198 (6), 963–969.
Jørgensen, P.B., Fenton, T.M., Mörbe, U.M., Riis, L.B., Jakobsen, H.L., Nielsen, O.H., Agace, W.W., 2021 Apr. Identification, isolation and analysis of human gut-associated lymphoid tissues. Nat. Protoc. 16 (4), 2051–2067.
Junt, T., Scandella, E., Ludewig, B., 2008 Oct. Form follows function: lymphoid tissue microarchitecture in antimicrobial immune defence. Nat. Rev. Immunol. 8 (10), 764–775.
Kanamori, Y., Ishimaru, K., Nanno, M., Maki, K., Ikuta, K., Nariuchi, H., Ishikawa, H., 1996 Oct 1. Identification of novel lymphoid tissues in murine intestinal mucosa where clusters of c-kit+ IL-7R+ Thy1+ lympho-hemopoietic progenitors develop. J. Exp. Med. 184 (4), 1449–1459.
Kararli, T.T., 1995 Jul. Comparison of the gastrointestinal anatomy, physiology, and biochemistry of humans and commonly used laboratory animals. Biopharm Drug Dispos. 16 (5), 351–380.
Katakai, T., Hara, T., Lee, J.H., Gonda, H., Sugai, M., Shimizu, A., 2004 Aug. A novel reticular stromal structure in lymph node cortex: an immuno-platform for interactions among dendritic cells, T cells and B cells. Int. Immunol. 16 (8), 1133–1142.
Kiss, E.A., Vonarbourg, C., Kopfmann, S., Hobeika, E., Finke, D., Esser, C., Diefenbach, A., 2011. Natural aryl hydrocarbon receptor ligands control organogenesis of intestinal lymphoid follicles. Science 334, 1561–1565.
Levast, B., De Monte, M., Melo, S., Chevaleyre, C., Berri, M., Salmon, H., Meurens, F., 2010 Feb. Differences in transcriptomic profile and IgA repertoire between jejunal and ileal Peyer's patches. Dev. Comp. Immunol. 34 (2), 102–106.
Liebler-Tenorio, E.M., Pabst, R., May-Jun 2006. MALT structure and function in farm animals. Vet. Res. 37 (3), 257–280.
Luppi, A., 2017 Aug 8. Swine enteric colibacillosis: diagnosis, therapy and antimicrobial resistance. Porcine Health Manag 3, 16.
Magri, G., Comerma, L., Pybus, M., Sintes, J., Lligé, D., Segura-Garzón, D., Bascones, S., Yeste, A., Grasset, E.K., Gutzeit, C., Uzzan, M., Ramanujam, M., van Zelm, M.C., Albero-González, R., Vazquez, I., Iglesias, M., Serrano, S., Márquez, L., Mercade, E., Mehandru, S., Cerutti, A., 2017 Jul 18. Human secretory IgM emerges from plasma cells clonally related to gut memory B cells and targets highly diverse commensals. Immunity 47 (1), 118–134.e8.
Makala, L.H., Kamada, T., Nishikawa, Y., Nagasawa, H., Igarashi, I., Fujisaki, K., Suzuki, N., Mikami, T., Haverson, K., Bailey, M., Stokes, C.R., Bland, P.W., 2000. Ontogeny of pig discrete Peyer's patches: distribution and morphometric analysis. Pathobiology 68 (6), 275–282.
Mansfield, L.S., Gauthier, D.T., 2004 Oct. Lymphoglandular complexes are important colonic sites for immunoglobulin A induction against Campylobacter jejuni in a swine disease model. Comp. Med. 54 (5), 514–523.
Martinoli, C., Chiavelli, A., Rescigno, M., 2007 Dec. Entry route of Salmonella typhimurium directs the type of induced immune response. Immunity 27 (6), 975–984.
McCance, R.A., 1974 Jul. The effect of age on the weights and lengths of pigs' intestines. J. Anat. 117 (Pt 3), 475–479.
Meurens, F., Summerfield, A., Nauwynck, H., Saif, L., Gerdts, V., 2012 Jan. The pig: a model for human infectious diseases. Trends Microbiol. 20 (1), 50–57.
Moghaddami, M., Cummins, A., Mayrhofer, G., 1998 Dec. Lymphocyte-filled villi: comparison with other lymphoid aggregations in the mucosa of the human small intestine. Gastroenterology 115 (6), 1414–1425.
Mörbe, U.M., Jørgensen, P.B., Fenton, T.M., von Burg, N., Riis, L.B., Spencer, J., Agace, W.W., 2021 Jul. Human gut-associated lymphoid tissues (GALT); diversity, structure and function. Mucosal Immunol. 14 (4), 793–802.
Morfitt, D.C., Pohlenz, J.F., 1989 Jan. Porcine colonic lymphoglandular complex: distribution, structure, and epithelium. Am. J. Anat. 184 (1), 41–51.
Nagai, S., Mimuro, H., Yamada, T., Baba, Y., Moro, K., Nochi, T., Kiyono, H., Suzuki, T., Sasakawa, C., Koyasu, S., 2007 May 22. Role of Peyer's patches in the induction of Helicobacter pylori-induced gastritis. Proc Natl Acad Sci U S A 104 (21), 8971–8976.
Pabst, R., 2020 May. The pig as a model for immunology research. Cell Tissue Res. 380 (2), 287–304.
Pabst, R., Geist, M., Rothkötter, H.J., Fritz, F.J., 1988 Jul. Postnatal development and lymphocyte production of jejunal and ileal Peyer's patches in normal and gnotobiotic pigs. Immunology 64 (3), 539–544.
Pabst, O., Herbrand, H., Friedrichsen, M., Velaga, S., Dorsch, M., Berhardt, G., Worbs, T., Macpherson, A.J., Förster, R., 2006 Nov 15. Adaptation of solitary intestinal lymphoid tissue in response to microbiota and chemokine receptor CCR7 signaling. J. Immunol. 177 (10), 6824–6832.
Pescovitz, M.D., Sakopoulos, A.G., Gaddy, J.A., Husmann, R.J., Zuckermann, F.A., 1994 Oct. Porcine peripheral blood CD4+/CD8+ dual expressing T-cells. Vet. Immunol. Immunopathol. 43 (1–3), 53–62.
Rhouma, M., Fairbrother, J.M., Beaudry, F., Letellier, A., 2017 May 19. Post weaning diarrhea in pigs: risk factors and non-colistin-based control strategies. Acta Vet. Scand. 59 (1), 31.
Rothkötter, H.J., Sowa, E., Pabst, R., 2002 Sep-Oct. The pig as a model of developmental immunology. Hum. Exp. Toxicol. 21 (9–10), 533–536.
Russell, G.J., Bhan, A.K., Winter, H.S., 1990 Mar. The distribution of T and B lymphocyte populations and MHC class II expression in human fetal and postnatal intestine. Pediatr. Res. 27 (3), 239–244.
Schiavinato, A., Przyklenk, M., Kobbe, B., Paulsson, M., Wagener, R., 2021 Sep. Collagen type VI is the antigen recognized by the ER-TR7 antibody. Eur. J. Immunol. 51 (9), 2345–2347.
Senda, T., Dogra, P., Granot, T., Furuhashi, K., Snyder, M.E., Carpenter, D.J., Szabo, P.A., Thapa, P., Miron, M., Farber, D.L., 2019 Mar. Microanatomical dissection of human intestinal T-cell immunity reveals site-specific changes in gut-associated lymphoid tissues over life. Mucosal Immunol. 12 (2), 378–389.
Sinkora, M., Stepanova, K., Sinkorova, J., 2013 Apr. Different anti-CD21 antibodies can be used to discriminate developmentally and functionally different subsets of B lymphocytes in circulation of pigs. Dev. Comp. Immunol. 39 (4), 409–418.
Sinkora, M., Butler, J.E., Lager, K.M., Potockova, H., Sinkorova, J., 2014 Sep 4. The comparative profile of lymphoid cells and the T and B cell spectratype of germ-free piglets infected with viruses SIV, PRRSV or PCV2. Vet. Res. 45 (1), 91.
Skrzypek, T.H., Kazimierczak, W., Skrzypek, H., Valverde Piedra, J.L., Godlewski, M.M., Zabielski, R., 2018 Feb. Mechanisms involved in the development of the small intestine mucosal layer in postnatal piglets. J. Physiol. Pharmacol. 69 (1), 127–138.
Snoeck, V., Verfaillie, T., Verdonck, F., Goddeeris, B.M., Cox, E., 2006 May 1. The jejunal Peyer's patches are the major inductive sites of the F4-specific immune response following intestinal immunisation of pigs with F4 (K88) fimbriae. Vaccine 24 (18), 3812–3820.
Spencer, J., Klavinskis, L.S., Fraser, L.D., 2012 May 11. The human intestinal IgA response; burning questions. Front. Immunol. 3, 108.

Stokes, C.R., 2017 Jan 26. The development and role of microbial-host interactions in gut mucosal immune development. J. Anim. Sci. Biotechnol. 8, 12.
Tsuji, M., Suzuki, K., Kitamura, H., Maruya, M., Kinoshita, K., Ivanov, I.I., Itoh, K., Littman, D.R., Fagarasan, S., 2008 Aug 15. Requirement for lymphoid tissue-inducer cells in isolated follicle formation and T cell-independent immunoglobulin A generation in the gut. Immunity 29 (2), 261–271.
Veiga-Fernandes, H., Coles, M.C., Foster, K.E., Patel, A., Williams, A., Natarajan, D., Barlow, A., Pachnis, V., Kioussis, D., 2007 Mar 29. Tyrosine kinase receptor RET is a key regulator of Peyer's Patch organogenesis. Nature 446 (7135), 547–551.
Van Vliet, E., Melis, M., Foidart, J.M., Van Ewijk, W., 1986 Jul. Reticular fibroblasts in peripheral lymphoid organs identified by a monoclonal antibody. J. Histochem. Cytochem. 34 (7), 883–890.
Xu, R.J., Mellor, D.J., Tungthanathanich, P., Birtles, M.J., Reynolds, G.W., Simpson, H. V., 1992 Oct. Growth and morphological changes in the small and the large intestine in piglets during the first three days after birth. J. Dev. Physiol. 18 (4), 161–172.
Yaeger, M., Funk, N., Hoffman, L., 2002 Jul. A survey of agents associated with neonatal diarrhea in Iowa swine including Clostridium difficile and porcine reproductive and respiratory syndrome virus. J. Vet. Diagn. Invest. 14 (4), 281–287.
Yang, H., Parkhouse, R.M., 1996 Sep. Phenotypic classification of porcine lymphocyte subpopulations in blood and lymphoid tissues. Immunology 89 (1), 76–83.
Zhao, Y., Uduman, M., Siu, J.H.Y., Tull, T.J., Sanderson, J.D., Wu, Y.B., Zhou, J.Q., Petrov, N., Ellis, R., Todd, K., Chavele, K.M., Guesdon, W., Vossenkamper, A., Jassem, W., D'Cruz, D.P., Fear, D.J., John, S., Scheel-Toellner, D., Hopkins, C., Moreno, E., Woodman, N.L., Ciccarelli, Heck S., Kleinstein, S.H., M14, Bemark, Spencer, J., 2018 Sep 21. Spatiotemporal segregation of human marginal zone and memory B cell populations in lymphoid tissue. Nat. Commun. 9 (1), 3857.
Zuckermann, F.A., Gaskins, H.R., 1996 Mar. Distribution of porcine CD4/CD8 double-positive T lymphocytes in mucosa-associated lymphoid tissues. Immunology 87 (3), 493–499.
Zuckermann, F.A., Husmann, R.J., 1996 Mar. Functional and phenotypic analysis of porcine peripheral blood CD4/CD8 double-positive T cells. Immunology 87 (3), 500–512.